Electronic Supplementary Material (ESI) for Physical Chemistry Chemical Physics.

Dissecting the species-specific recognition of Neoseptin 3 by TLR4/MD2 via molecular dynamics simulations

Siru Wu,[ab] Cong Zhang,[ab] Yibo Wang,[a] Penghui Li,[c] Xiubo Du,[c] and Xiaohui Wang*[abd]

[a]Laboratory of Chemical Biology, Changchun Institute of Applied Chemistry, Chinese Academy of Sciences, Changchun, Jilin, 130022, China
[b]School of Applied Chemistry and Engineering, University of Science and Technology of China, Hefei, Anhui, 230026, China
[c]Shenzhen Key Laboratory of Marine Biotechnology and Ecology, College of Life Sciences and Oceanography, Shenzhen University, Shenzhen, Guangdong, 518060, China
[d]Beijing National Laboratory for Molecular Sciences, Beijing, 100190, China

Corresponding Author
Xiaohui Wang, Email: xiaohui.wang@ciac.ac.cn

Supporting Information

Table S1 Summary of protein sequence alignment of TLR4 and MD2 between mouse and human. Comparison and alignment of mouse and human sequences were conducted via pairwise sequence alignment in EMBL-EBI[1].

	Length	Identity	Similarity	Gap
TLR4	1-827	559/827(67.6%)	660/827(79.8%)	4/827(0.5%)
MD2	1-160	103/160(64.4%)	129/160(80.6%)	0/160(0.0%)

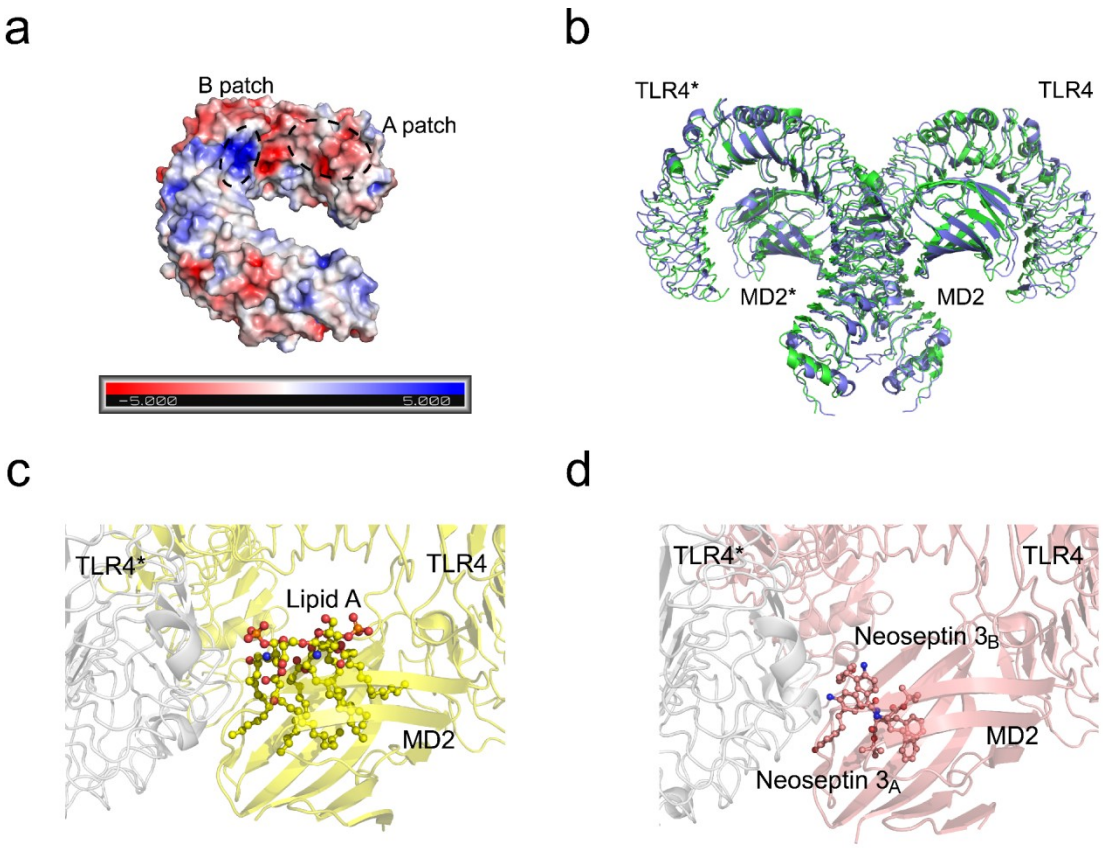

Fig. S1 (a) A patch and B patch[2] of mouse TLR4 extracted from mouse (TLR4/MD2/2*Neoseptin 3)$_2$ heterotetramer (PDB ID: 5IJC[3]); (b) Structural comparison of mouse TLR4/MD2 (green, PDB ID: 5IJD[3]) and human TLR4/MD2 (blue, PDB ID: 3FXI[4]); (c) Position of lipid A in human (TLR4/MD2/Lipid A)$_2$ (PDB ID: 3FXI[4]); (d) Position of Neoseptin 3 in mouse (TLR4/MD2/2*Neoseptin 3)$_2$ (PDB ID: 5IJC[3]). Electrostatic potentials of TLR4 were calculated via APBS program[5] and displayed with PyMol software[6]. Protein was shown as cartoon and ligands were shown as ball-stick models.

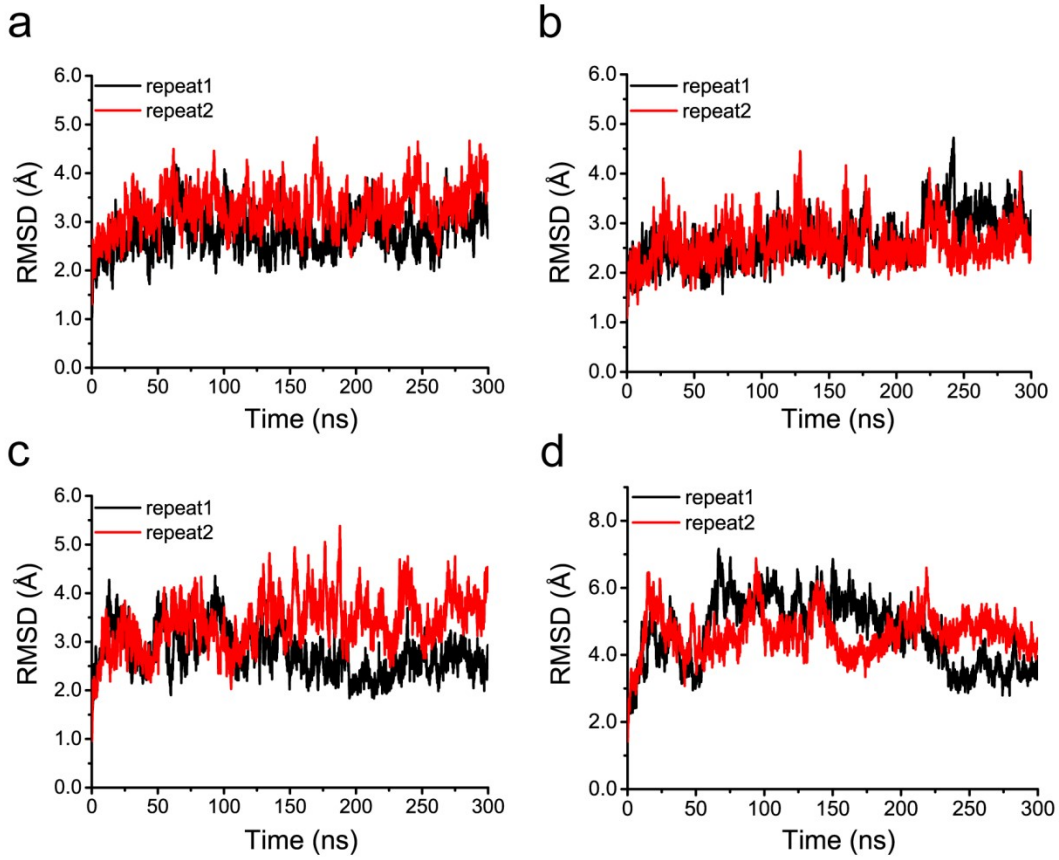

Fig. S2 RMSDs of the protein backbone during the repeated simulation of $(TLR4/MD2)_2$ from mouse (a, b) or human (c, d) complexed with lipid A (a, c) or Neoseptin 3 (b, d).

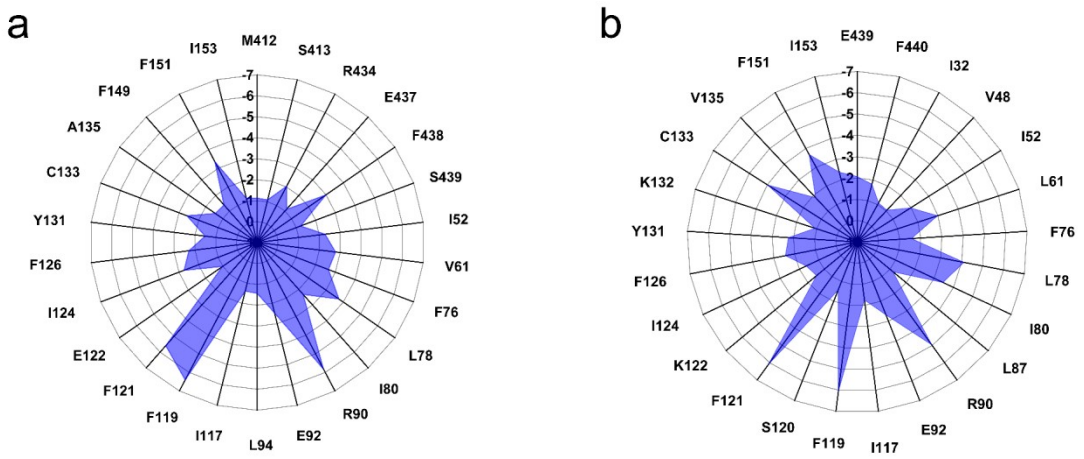

Fig. S3 Main residues' contributions to the binding of Neoseptin 3 with mouse TLR4/MD2 (a) and human TLR4/MD2 (b) after the energy decomposition of binding free energies. Unit: kcal/mol.

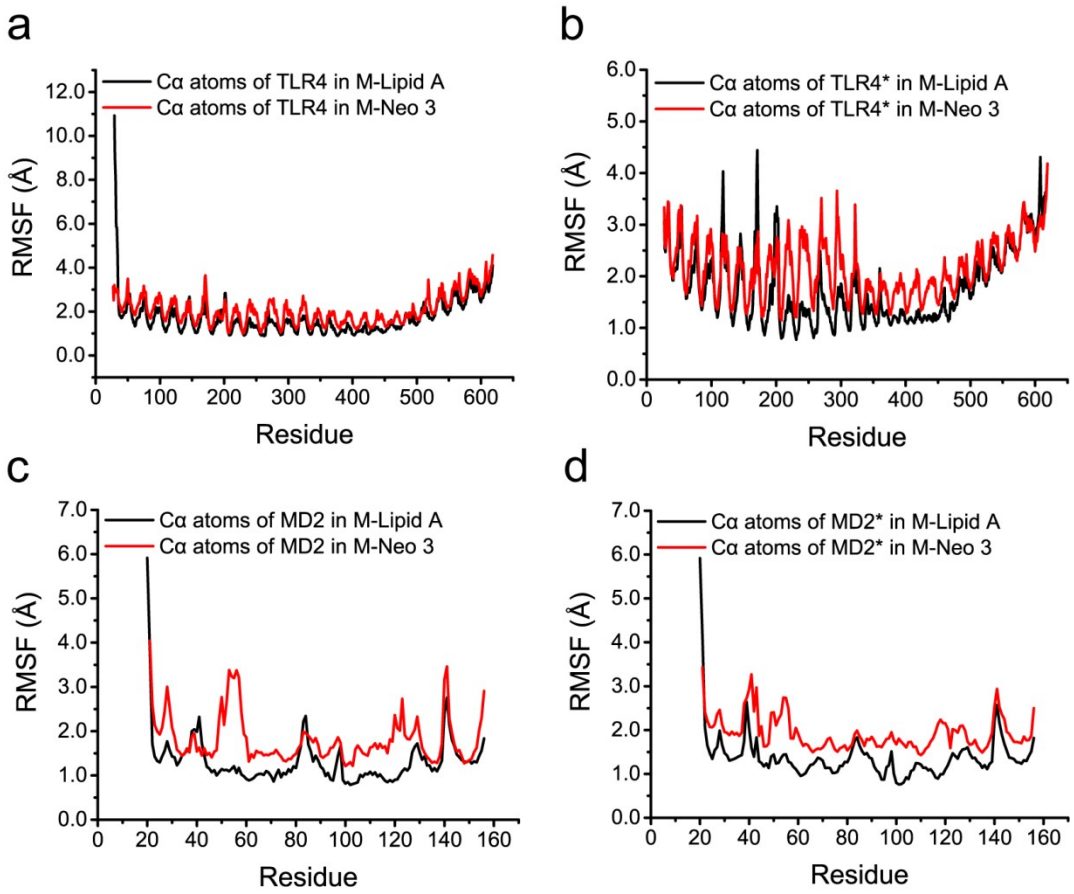

Fig. S4 RMSF of Cα atoms of mouse TLR4 (a), TLR4* (b), MD2 (c), and MD2* (d) when bound with lipid A or Neoseptin 3. All replicates of each system were merged together, and the RMSFs were calculated with the merged trajectories for the last 50 ns.

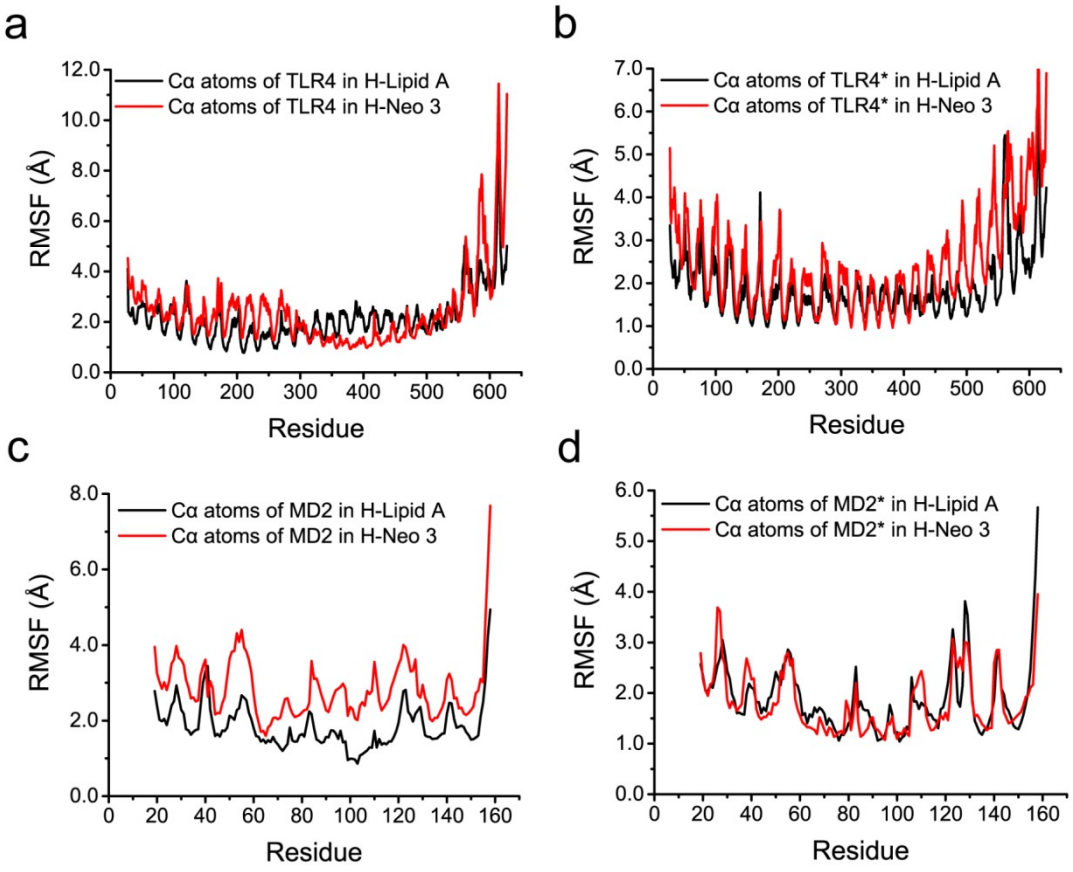

Fig. S5 RMSF of Cα atoms of human TLR4 (a), TLR4* (b), MD2 (c), and MD2* (d) when bound with lipid A or Neoseptin 3. All replicates of each system were merged together, and the RMSFs were calculated with the merged trajectories for the last 50 ns.

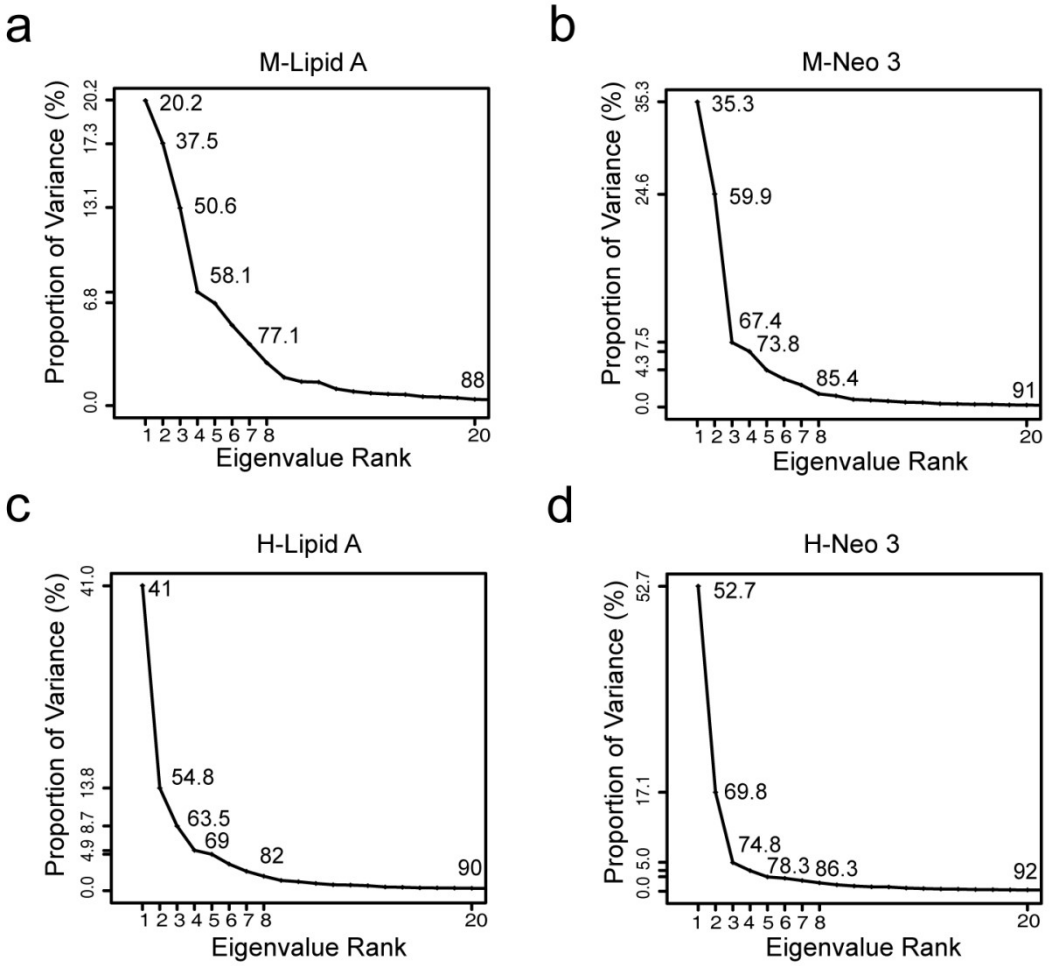

Fig. S6 Proportion of variance captured by principal components for mouse (TLR4/MD2/Lipid A)$_2$ (a), mouse (TLR4/MD2/2*Neoseptin 3)$_2$ (b), human (TLR4/MD2/Lipid A)$_2$ (c) and human (TLR4/MD2/2*Neoseptin 3)$_2$ (d).

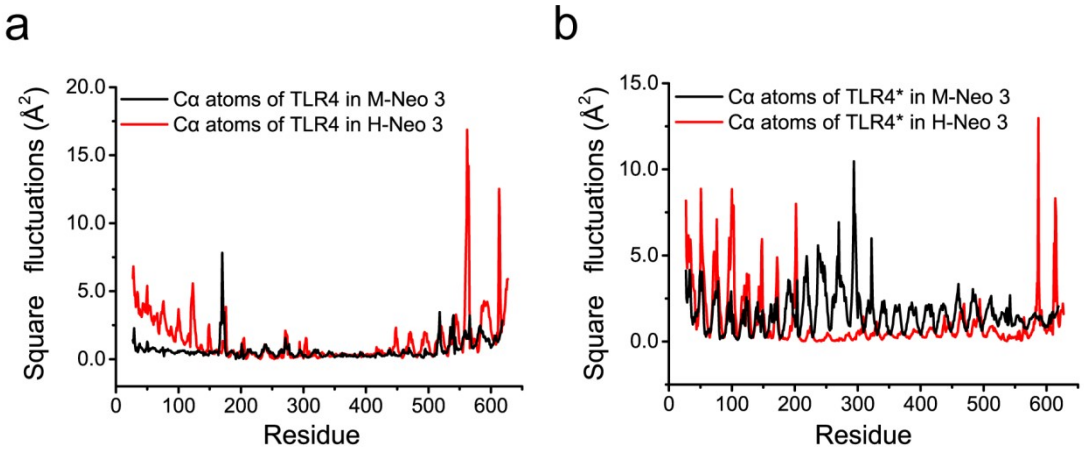

Fig. S7 The square fluctuations of the second mode of TLR4 (a) or TLR4* (b) bound with Neoseptin 3.

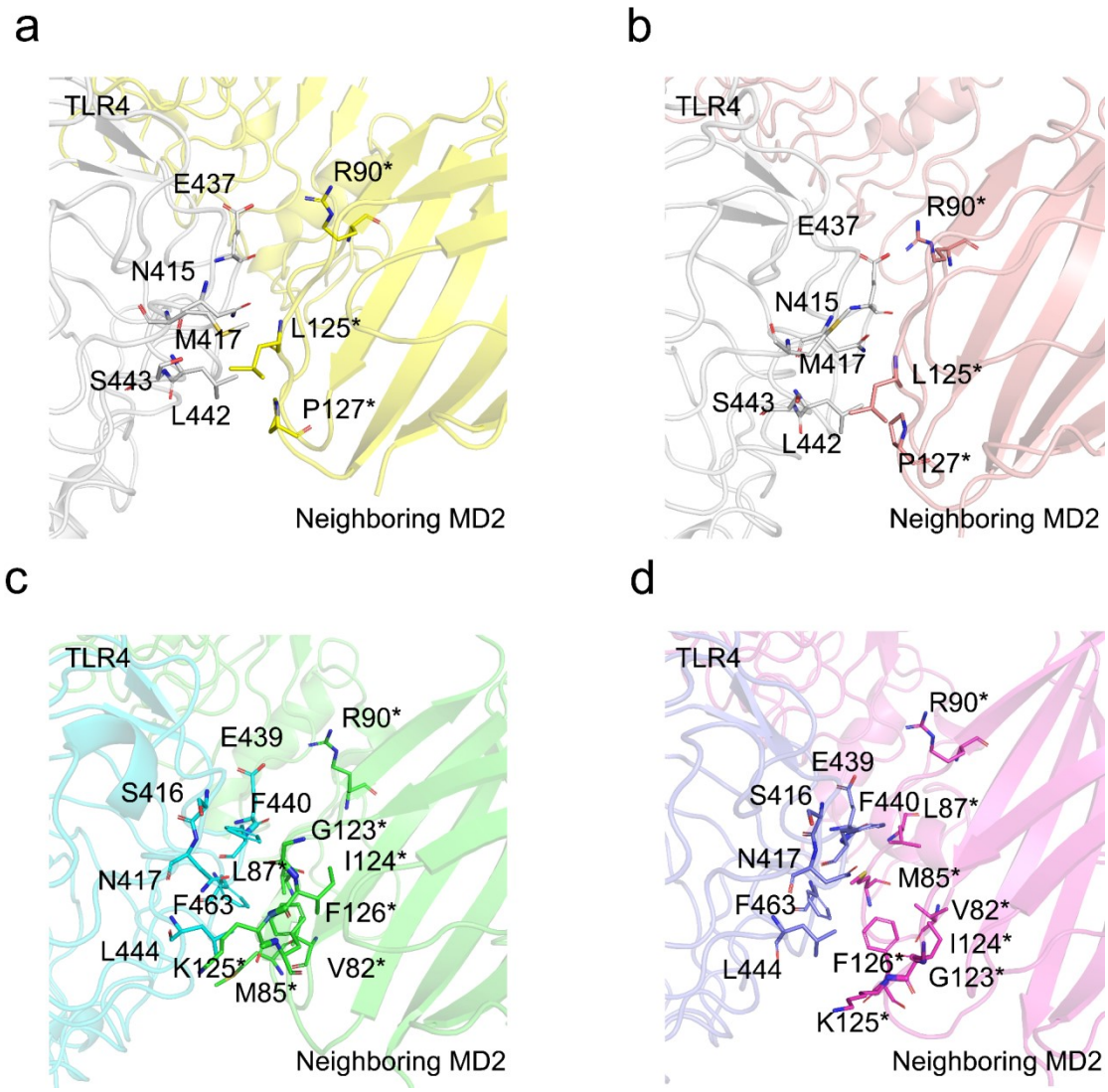

Fig. S8 Representative conformations and positions of key residues involved in the hydrophobic interactions and hydrogen bonds between TLR4 and neighboring MD2 of mouse $(TLR4/MD2/Lipid\ A)_2$ (a), mouse $(TLR4/MD2/2*Neoseptin\ 3)_2$ (b), human $(TLR4/MD2/Lipid\ A)_2$ (c), and human $(TLR4/MD2/2*Neoseptin\ 3)_2$ (d). Protein was shown as cartoon and ligands were not shown for clarity. Residues of neighboring MD2 were shown as sticks and labeled with asterisks.

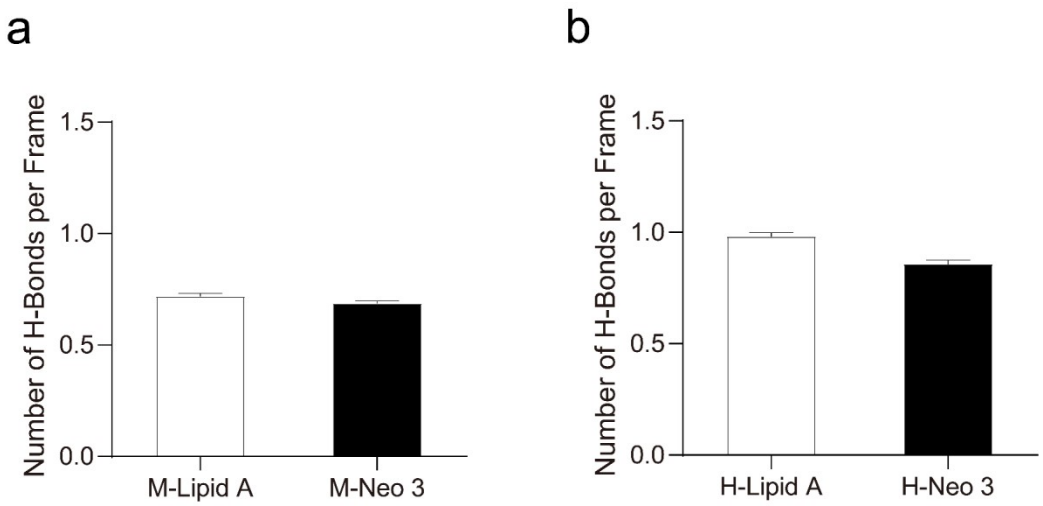

Fig. S9 Number of hydrogen bonds per frame between TLR4 and neighboring MD2 (including TLR4-MD2* and TLR4*-MD2) for mouse (a) or human (b) $(TLR4/MD2)_2$ interacting with lipid A and Neoseptin 3. All trajectories of replicates for each system were calculated. The data are shown as the mean ± SEM over the last 50 ns of simulations.

References

1. F. Madeira, M. Pearce, A. R. N. Tivey, P. Basutkar, J. Lee, O. Edbali, N. Madhusoodanan, A. Kolesnikov and R. Lopez, *Nucleic Acids Res*, 2022, **50**, W276-W279.
2. H. M. Kim, B. S. Park, J. I. Kim, S. E. Kim, J. Lee, S. C. Oh, P. Enkhbayar, N. Matsushima, H. Lee, O. J. Yoo and J. O. Lee, *Cell*, 2007, **130**, 906-917.
3. Y. Wang, L. Su, M. D. Morin, B. T. Jones, L. R. Whitby, M. M. Surakattula, H. Huang, H. Shi, J. H. Choi, K. W. Wang, E. M. Moresco, M. Berger, X. Zhan, H. Zhang, D. L. Boger and B. Beutler, *Proc Natl Acad Sci U S A*, 2016, **113**, E884-E893.
4. B. S. Park, D. H. Song, H. M. Kim, B. S. Choi, H. Lee and J. O. Lee, *Nature*, 2009, **458**, 1191-1195.
5. E. Jurrus, D. Engel, K. Star, K. Monson, J. Brandi, L. E. Felberg, D. H. Brookes, L. Wilson, J. Chen, K. Liles, M. Chun, P. Li, D. W. Gohara, T. Dolinsky, R. Konecny, D. R. Koes, J. E. Nielsen, T. Head-Gordon, W. Geng, R. Krasny, G.-W. Wei, M. J. Holst, J. A. McCammon and N. A. Baker, *Protein Science*, 2018, **27**, 112-128.
6. PyMol, *Schrödinger, LLC*, **Version 2.5.0a0**.